Journal Name

Dynamic Article Links ►

Cite this: DOI: 10.1039/c0xx00000x

www.rsc.org/xxxxxx

COMMUNICATION

Electronic Supplementary Information

`

Assembling CdSe/ZnS Core-Shell Quantum Dots on Localized DNA Nanostructures†

Junwye Lee,[a] Jongtaek Lee,[b] Sung Mo Yeon,[b] Sunmin Min,[b] Jinwoo Kim,[b] Hyeokwoo Choi,[b] Sunho Kim,[b] Jonghyun Koo,[b] Kyungseob Kim,[b] Sung Ha Park,*[a] Yonghan Roh*[b]

[a]*Sungkyunkwan Advanced Institute of Nanotechnology (SAINT) and Department of Physics, Sungkyunkwan University, Suwon 440-746, Korea.*
[b]*Sungkyunkwan Advanced Institute of Nanotechnology (SAINT) and School of Information & Communication Engineering, Sungkyunkwan University, Suwon 440-746, Korea.*

Fig. S1. CdSe/ZnS core-shell quantum dot (Qdot) analysis. (a) TEM image of Qdots with 3.71 ± 0.44 nm average particle size. (b) Energy dispersive X-ray spectrometry (EDS) spectra.

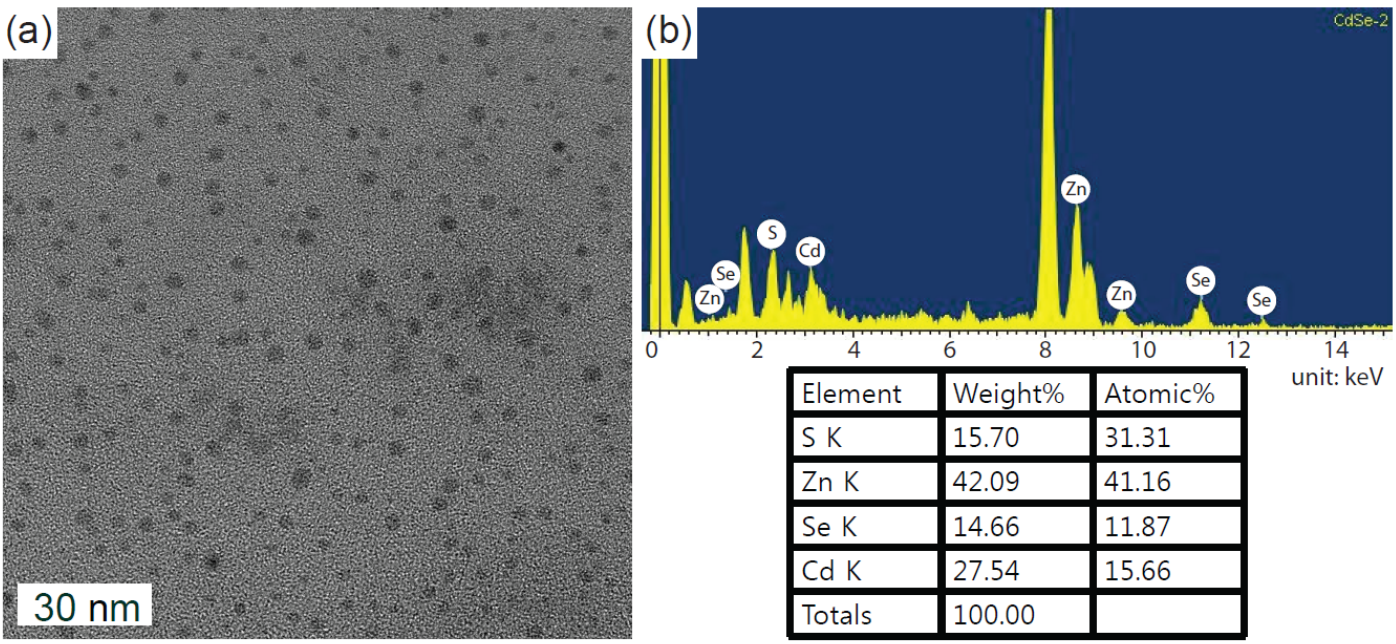

Element	Weight%	Atomic%
S K	15.70	31.31
Zn K	42.09	41.16
Se K	14.66	11.87
Cd K	27.54	15.66
Totals	100.00	

Fig. S2. Optical and Zeta-potential analyses for Qdots. (a) A Fourier transformed infra-red spectroscopy (FT-IR) spectrum of Qdots. The FT-IR spectrum shows a decrease of the peak of the P=O bond, while an amine peak was dramatically increased by ligand exchange from TOPO to DMAET. (b) A Zeta-potential analysis of DMAET-capped Qdots. The cationic DMAET ligands give about 32.11 mV of surface charge to Qdots. (c, d) UV-visible and photoluminescence (PL) spectra of both TOPO- and DMAET-capped Qdots. Peak shift in absorption spectroscopy in (c) resulted from a redistribution of the electronic density and increase of the energy of the Qdots attributed to the stronger Zn-thiol bond compared to the Zn-amine bond (C. Woelfle and R. O. Claus, *Nanotechnology*, 2007, **18**, 025402). Peak shift of PL spectrum and quenching of the fluorescence in (d) resulted from trapping of the photogenerated holes on the thiol groups, which hindered the radioactive recombination of the exciton.

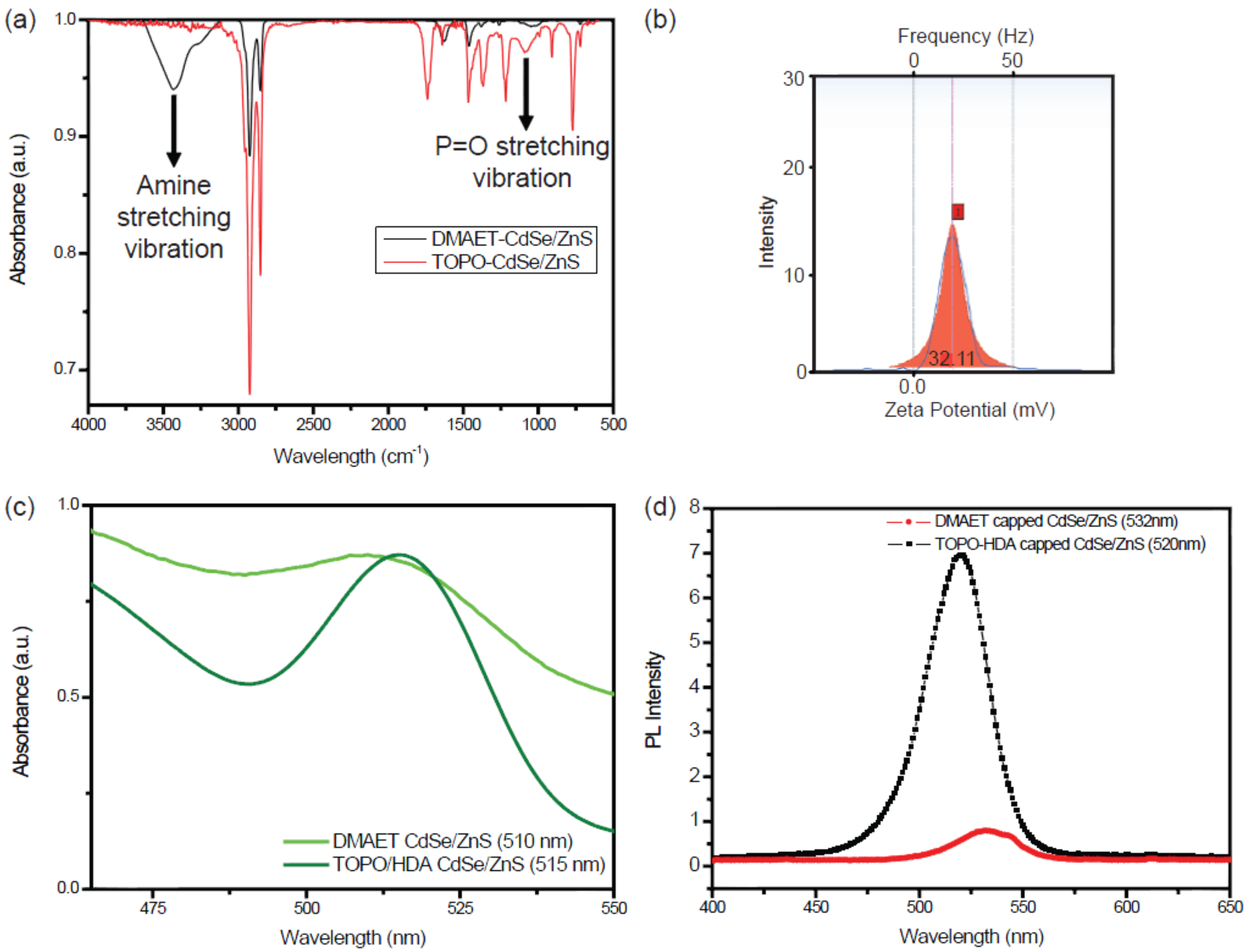

Fig. S3. Schematic illustrations and a sequence map of the double-crossover (DX) DNA lattice.

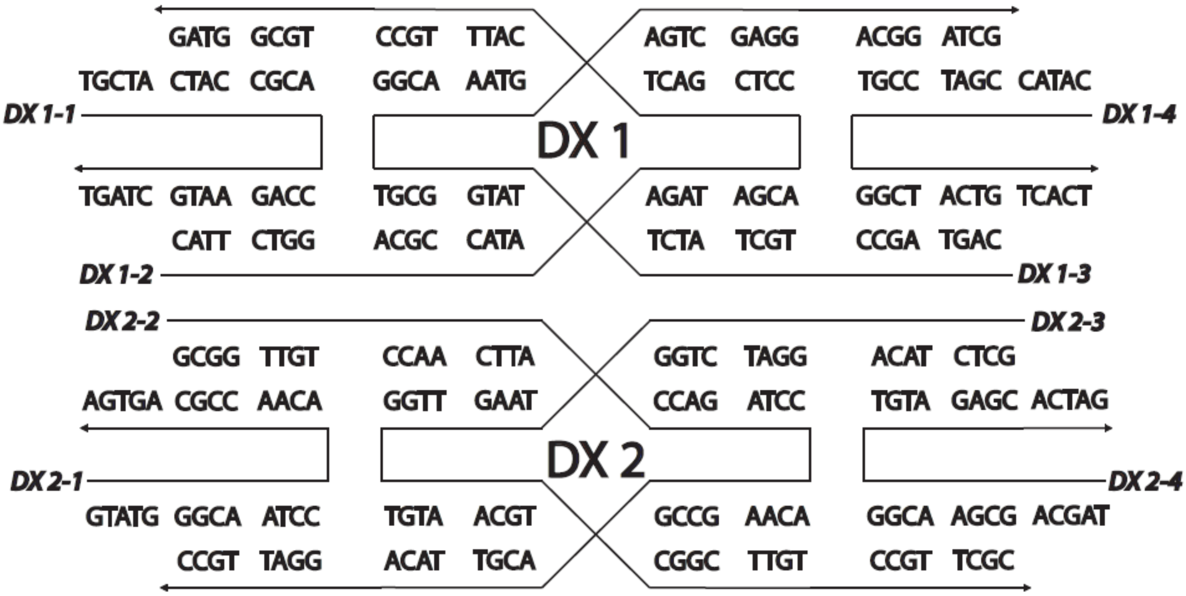

Strand name	Number of nucleotides	Sequence (5' to 3')
DX1-1	26	TGCTA CTACCGCA CCAGAATG CTAGT
DX1-2	48	CATTCTGG ACGCCATA AGATAGCA CCTCGACT CATTTGCC TGCGGTAG
DX1-3	48	CAGTAGCC TGCTATCT TATGGCGT GGCAAATG AGTCGAGG ACGGATCG
DX1-4	26	CATAC CGATCCGT GGCTACTG TCACT
DX2-1	26	GTATG GGCAATCC ACAACCGC AGTGA
DX2-2	48	GCGGTTGT CCAACTTA CCAGATCC ACAAGCCG ACGTTACA GGATTGCC
DX2-3	48	GCTCTACA GGATCTGG TAAGTTGG TGTAACGT CGGCTTGT CCGTTCGC
DX2-4	26	TAGCA GCGAACGG TGTAGAGC ACTAG

Fig. S4. Schematic illustrations and a sequence map of 5 helix ribbon (5 HR) and 8 helix tube (8 HT) nanostructures.

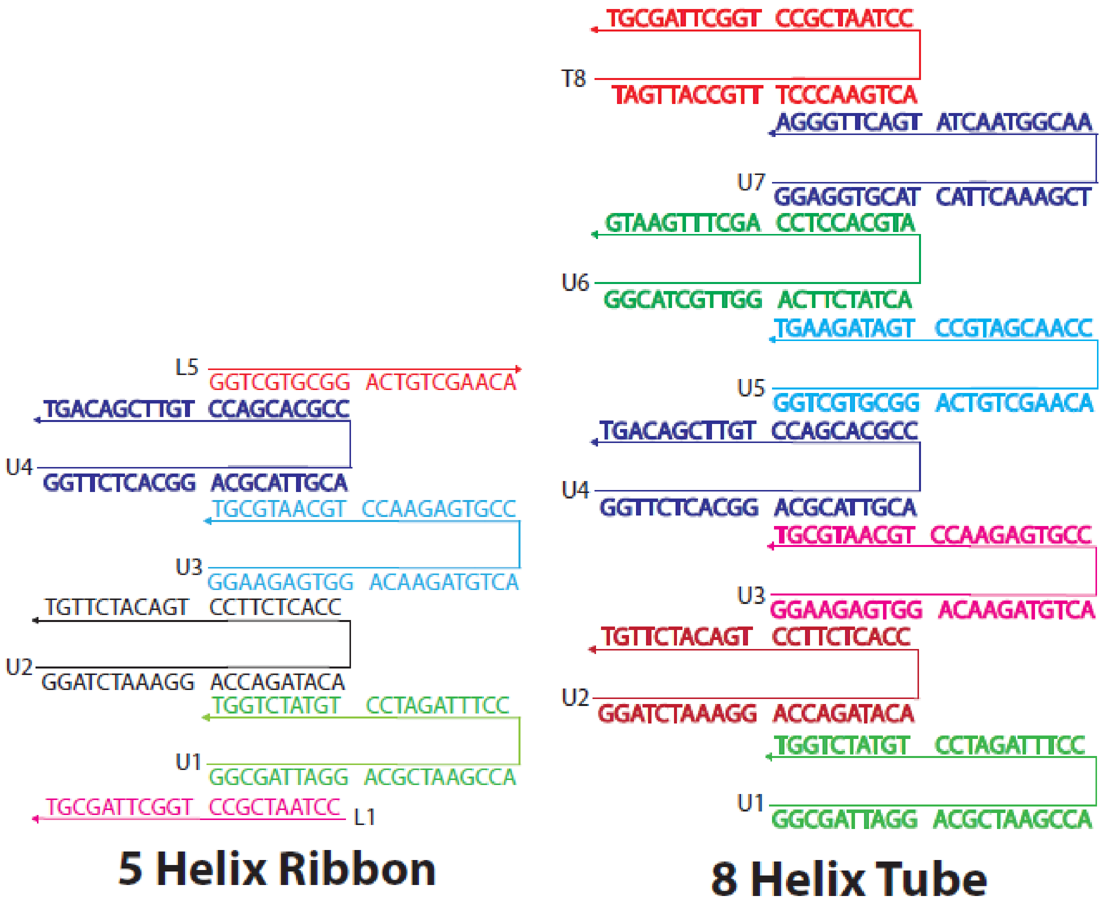

Strand name	Number of nucleotides	Sequence (5' to 3')
U1	42	GGCG ATTA GGAC GCTA AGCC ACCT TTAG ATCC TGTA TCTG GT
U2	42	GGAT CTAA AGGA CCAG ATAC ACCA CTCT TCCT GACA TCTT GT
U3	42	GGAA GAGT GGAC AAGA TGTC ACCG TGAG AACC TGCA ATGC GT
U4	42	GGTT CTCA CGGA CGCA TTGC ACCG CACG ACCT GTTC GACA GT
U5	42	GGTC GTGC GGAC TGTC GAAC ACCA ACGA TGCC TGAT AGAA GT
U6	42	GGCA TCGT TGGA CTTC TATC AATG CACC TCCA GCTT TGAA TG
U7	42	GGAG GTGC ATCA TTCA AAGC TAAC GGTA ACTA TGAC TTGG GA
L1	21	CCTA ATCG CCTG GCTT AGCGT
L5	21	GGTC GTGC GGAC TGTC GAACA
T8	42	TAGT TACC GTTT CCCA AGTC ACCT AATC GCCT GGCT TAGC GT

Fig. S5. TEM images of Qdots assembled on various DNA templates.

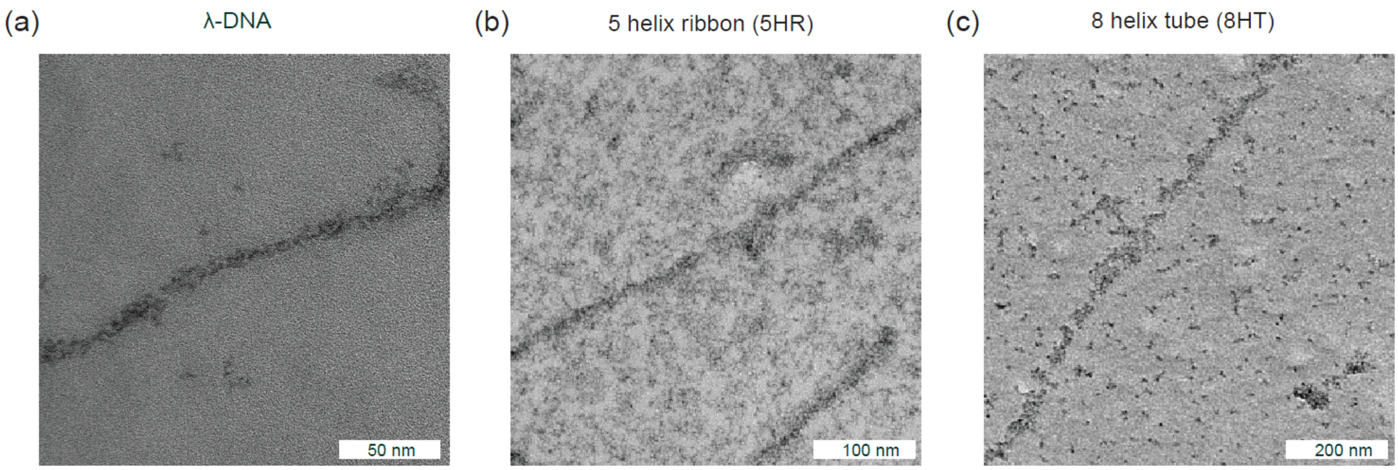

Fig. S6. Adsorption ratio analysis for Qdots on various DNA templates. The adsorption ratio was obtained by contrast analysis ($\frac{pixels\ for\ Qdots}{total\ pixels}$) of Qdots in SEM images.

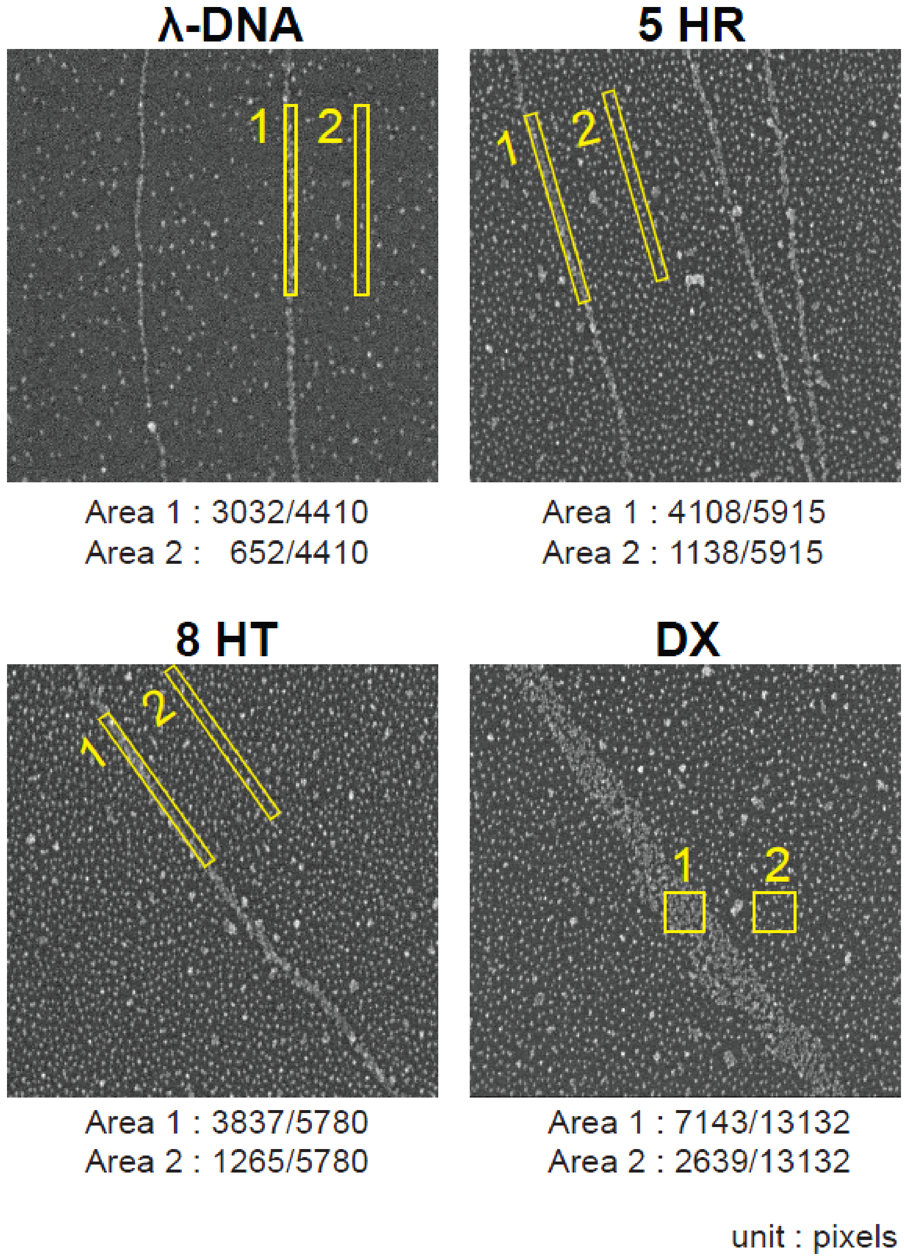

Fig. S7. Adsorption ratio analysis for Qdots on DNA templates fabricated by the SAG method on OTS-coated SiO_2 substrate. The adsorption ratio was obtained by contrast analysis ($\frac{pixels\ for\ Qdots}{total\ pixels}$) of Qdots in SEM images.

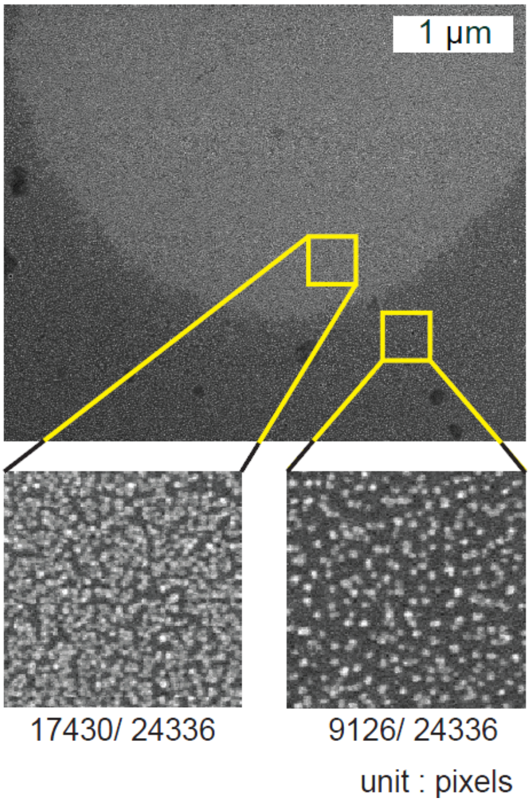

Fig. S8. Roughness analysis of bare and OTS-coated p-SiO_2 substrates.